Appendix

Towards natural care products: structural and deposition studies of bio-based polymer and surfactant mixtures

Alessandra Del Giudice,[a§] Marta Gubitosi,[b§*] Adrien Sthoer,[b] Sebastian Köhler,[c] Sophie Ayscough,[d] Maximilian W. A. Skoda,[e] Tommy Nylander,[c,d,f,g] Tobias Halthur[b,h,i]

[a]*Sapienza University of Rome, P.le A. Moro 5, 00185 Rome, Italy*
[b]*CR Competence AB, POBox 124, SE-221 00 Lund, Sweden*
[c]*LINXS Institute of Advanced Neutron and X-ray Science, Lund, Sweden*
[d]*Division of Physical Chemistry, Lund University, POBox 124, SE-221 00 Lund, Sweden*
[e]*ISIS Neutron and Muon Source, Harwell Science and Innovation Campus, Didcot OX110QX, U.K.*
[f]*NanoLund, Lund University, Lund, Sweden*
[g]*School of Chemical Engineering and Translational Nanobioscience Research Center, Sungkyunkwan University, Suwon 16419, Republic of Korea*
[h]*Biomedical Science, Faculty of Health and Society, Malmö University, SE-205 06 Malmö, Sweden*
[i]*Biofilms – Research Center for Biointerfaces (BRCB), Malmö University, SE-205 06 Malmö, Sweden.*

[§]*These authors equally contributed to the work*

Corresponding author:
marta@crcom.se

Supporting methods

SAXS models for NaC10 micelles. The core-shell sphere model for surfactant micelles involves highly correlated parameters (the Scattering Length Density - SLD - of core and shell domains with their relative size, and the absolute SLD values with the micelle concentration) [1]. It is therefore necessary to check the consistency of the best-fit parameters with the molecular model and the known sample concentrations. The known concentration of surfactant should let us estimate the expected volume fraction of aggregated objects in the sample.

One possible approach is to assume the macroscopic partial molar volume of NaC10 reported in the literature for the micellar form (175.0 cm^3/mol [2]) to approximately convert the mass concentration into volume fraction, and thus subtract the free surfactant concentration assumed equal to the CMC. The CMC has been assessed to be 1 wt% by the SAXS dilution series in the Tris buffer 20 mM pH 9 and in the presence of 0.09 M NaCl), and such value compares well to those reported in the literature for the surfactant in pure water, *e.g.* 1.6 wt% [3] or 2 wt% [2]). The density of a 10 wt% solution of NaC10 in pure water – approximately equal to 0.01 mole fraction – is reported to be less than 1% different from assuming that 1 g is equal to 1 cm^3 or 1 ml [4]. In this assumption, micellar volume fractions expected for 10, 5, 2 wt% samples would be respectively 0.081, 0.036 and 0.009. In Figure A.1a the SAXS data have been scaled according to these values, showing clearly that neither the intensity of the lower q maximum (mostly affected by the inter-micellar interference) or the intensity and position of the higher q maximum (mostly related to the micellar form factor) are perfectly superimposable. In particular, if we consider the data at 5 wt% as a reference, the intensity in the lower q for the 10 wt% sample is much lower than expected, and it is a clear indication of the effect of destructive interference due to the inter-micellar spatial correlations. In addition, the secondary maximum at higher q slightly shifts to lower q values with increasing concentration, suggesting a slight change of the average micelle form factor with concentration.

Zemb and Charpin [1] reported combined SANS and SAXS data fitting for the lower analogue sodium octanoate at concentration 200 g/L, suggesting that for this surfactant the scattering profiles at all accessible concentrations are always due to a combination of micellar form factor and inter-particle structure factor, and they suggest that the parameter values reported in the literature based on SAXS data fitting only at the time were erroneous since neglected the interference effects. Imposing for the core and shell SLD values of $6.57 \cdot 10^{-4}$ nm^{-2} and $10.3 \cdot 10^{-4}$ nm^{-2} as reported for sodium octanoate [1], the best fit for NaC10 at 5 wt% gives a radius of the core of 1.35 nm and a shell thickness of 1.00 nm, also considering a volume fraction of 0.05 and the presence of inter-micellar interactions modelled by a Hayter-Penfold MSA structure factor with charge -7. Using the same SLD values for describing the SAXS data at 10 wt%, leads to a reasonable description of the secondary maximum position and height with similar core radius and shell thickness values (1.33 nm and 0.96 nm), but a much higher volume fraction of 0.167 (more than 3 times the value obtained for the 5 wt% sample). Such assumption also allows for reproducing the main oscillation in the SAXS profile collected at 2 wt% (results reported in Table A.2).

The experimental data for $q > 2.5$ nm^{-1} deviate from the simple form factor of a core-shell sphere and this could be for several reasons. First, the presence of free sodium decanoate at a relatively high concentration can give a contribution to the SAXS intensity in this region, as suggested by the experimental data collected for samples at concentration below 1.5 wt% (Figure 3a in the main text). In addition, even in the absence of free surfactant monomers in a significant amount the form factor of a simple geometrical solid might lose accuracy to reproduce the micelles at the single surfactant molecule resolution (for $q > 2.5$ nm^{-1}, the characteristic distances are < 2.5 nm) [5]. Introducing polydispersity or ellipticity of the micellar core sizes can usually improve the model, but in this context we decided as a first approach not to introduce additional parameters due to the low information content of the data in the low q region where the forward scattering is greatly suppressed due to both possible inter-particle interference and the low overall contrast of the micelles compared to the aqueous background, despite the well-defined contrast of the hydrophilic and counter-ion rich shell. An attempt to improve the fits presented in Figure 3a for NaC10 2% and 5% is presented in Figure A.1b: a background signal in the high q region was considered to account for the scattering due to free monomers (black dashed line), and, in addition, a deviation from the spherical shape of the micelle form factor (purple solid line) was assumed. The assumption of ellipsoidal shape rather than spherical shape improves indeed the agreement between model and data, whereas the introduction of polydispersity of core radius or shell thickness mainly reduces the depth of the minimum around 0.8 nm^{-1} but cannot change the shape of the high q portion of the secondary maximum ($q > 2.5$ nm^{-1}).

From the assumed value of the core SLD ($6.57 \cdot 10^{-4}$ nm^{-2} i.e. an electron density of 234 electrons/nm^3), considering the atomic composition of the $CH_3(CH_2)_8$- hydrophobic tails (73 electrons), a tail volume of 0.313 nm^3 can be estimated (compared with the estimate with the Tanford formula giving V_{tail} (nm^3) = 0.0274 + 0.0269 n_C = 0.270 nm^3), and the aggregation number can be calculated from the ratio between the core volume of the fit models and the individual tail volume.

Model-independent evaluation of SAXS data. To help the assignment of a q_{peak} value, the first derivative of the smoothed SAXS data was calculated with the Savitsky-Golay method implemented in Matlab. We assigned the maximum position to the q value at which the first derivative value crosses zero, and estimated error bars of ± 0.05 nm.
The estimate of the radius of gyration R_g and intensity extrapolated at zero angle $I(0)$ by means of the Guinier approximation was performed with the *datrg* tool of the ATSAS package [6] imposing the same q interval for all data (0.16-0.29 nm^{-1} or 0.66-1.1 nm^{-1}) or by using the *autorg* tool to automatically select the optimal interval for Guinier fit linearity for each experimental profile.

The indirect Fourier transform method implemented in the BayesApp code [7] was employed to obtain the pair distance distribution functions $P(r)$ allowing for negativity, together with additional estimates of R_g and $I(0)$.

For Quatin samples the molecular weight was estimated from the SAXS intensity $I(0)$ according to:

$$MW[Da] = \frac{I(q)[cm^{-1}]\cdot N_A[mol^{-1}]}{\Delta\rho_M^2[cm^2\cdot g^{-2}]\cdot c[g\cdot cm^{-3}]} \qquad \text{(eq. A1)}$$

$\Delta\rho_M^2$ is the squared scattering contrast per mass of polymer, which is obtained as:

$$\Delta\rho_M^2 = r_e(\rho_{M,dry} - \rho_{solv}\cdot\tilde{v}) \qquad \text{(eq. A2)}$$

where ρ_{solv} ($3.34\cdot10^{23}$ electrons/cm^3) is the electron density of the water solvent, $r_e = 2.8179\cdot10^{-13}$ cm is the scattering length of the electron, $\rho_{M,dry}$ in e/g is the number of electrons per mass of dry polymer, obtained from the chemical structure and known degree of cationic substitution, and $\tilde{v}$ is the partial specific volume of the polymer, estimated using an empirical method [8] and compared with an experimental value reported for inulin in water at 20 °C [9] (Table A.4a).

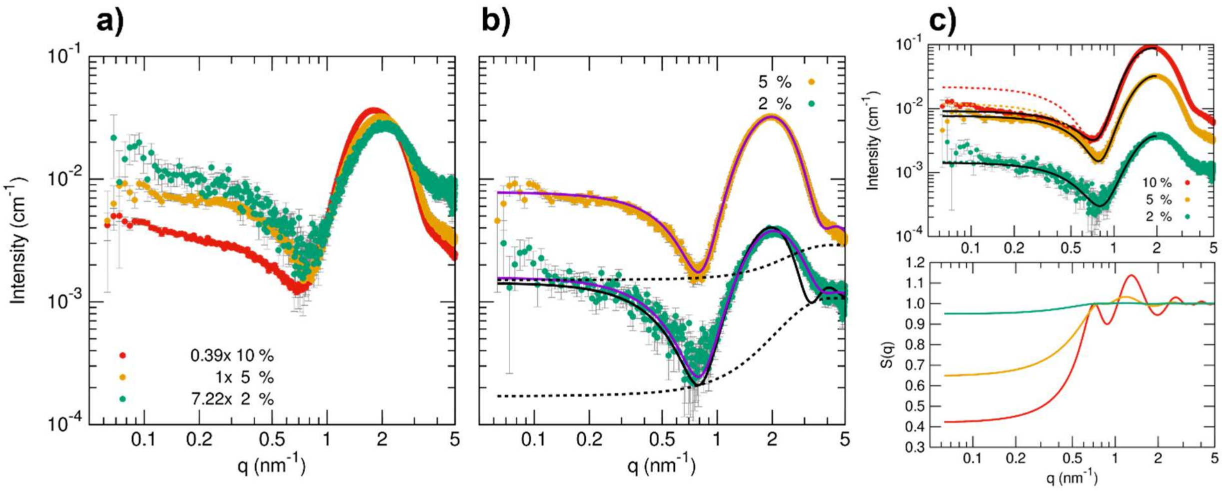

Figure A.1. *a) SAXS patterns of NaC10 samples at concentrations 10, 5 and 2 wt% at 25 °C scaled according to the calculated relative volume fraction of micelles taking the 5% sample as a reference. b) Modelling of the SAXS data from NaC10 micelles up to 5 nm^{-1}: background contribution from free NaC10 molecules modelled as a broad peak (dotted black lines), core-shell sphere including background contribution for the 2 wt% sample (black solid line), and core-shell ellipsoid models including background contribution for both 2 wt% and 5 wt% samples (purple solid lines). c) Model fits reported in Figure 2a of the main text (black lines) with highlight on the form factor and structure factor contributions: form factor contributions are reported as dashed colored lines, and in the panel below the structure factor contributions for the three NaC10 concentrations (colored solid lines) are obtained as the overall model intensity divided by the form factor.*

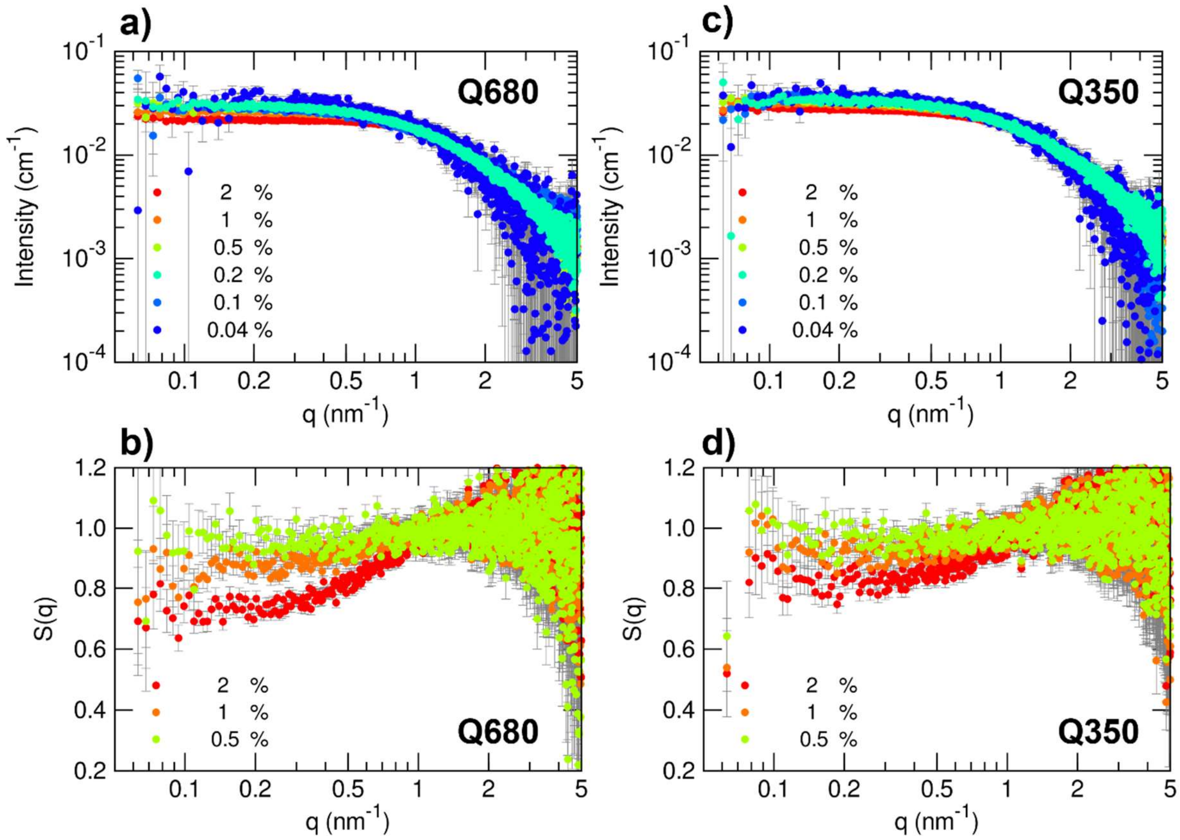

Figure A2. *a) SAXS patterns of Q680 samples at concentrations from 2 to 0.04 wt% at 25 °C scaled to the data for 1 wt% to optimize overlap in the q region 0.9-2.6 nm^{-1}. b) Estimate of the structure factor contribution to the scattering profiles for the most concentrated samples obtained as a point-by-point division of the I(q) of samples with polymer content > 0.2 wt% by the experimental I(q) for the sample at 0.2 wt%, assumed as coincident with the average form factor. The same is shown for the dilution series of Q350 in panels c) and d).*

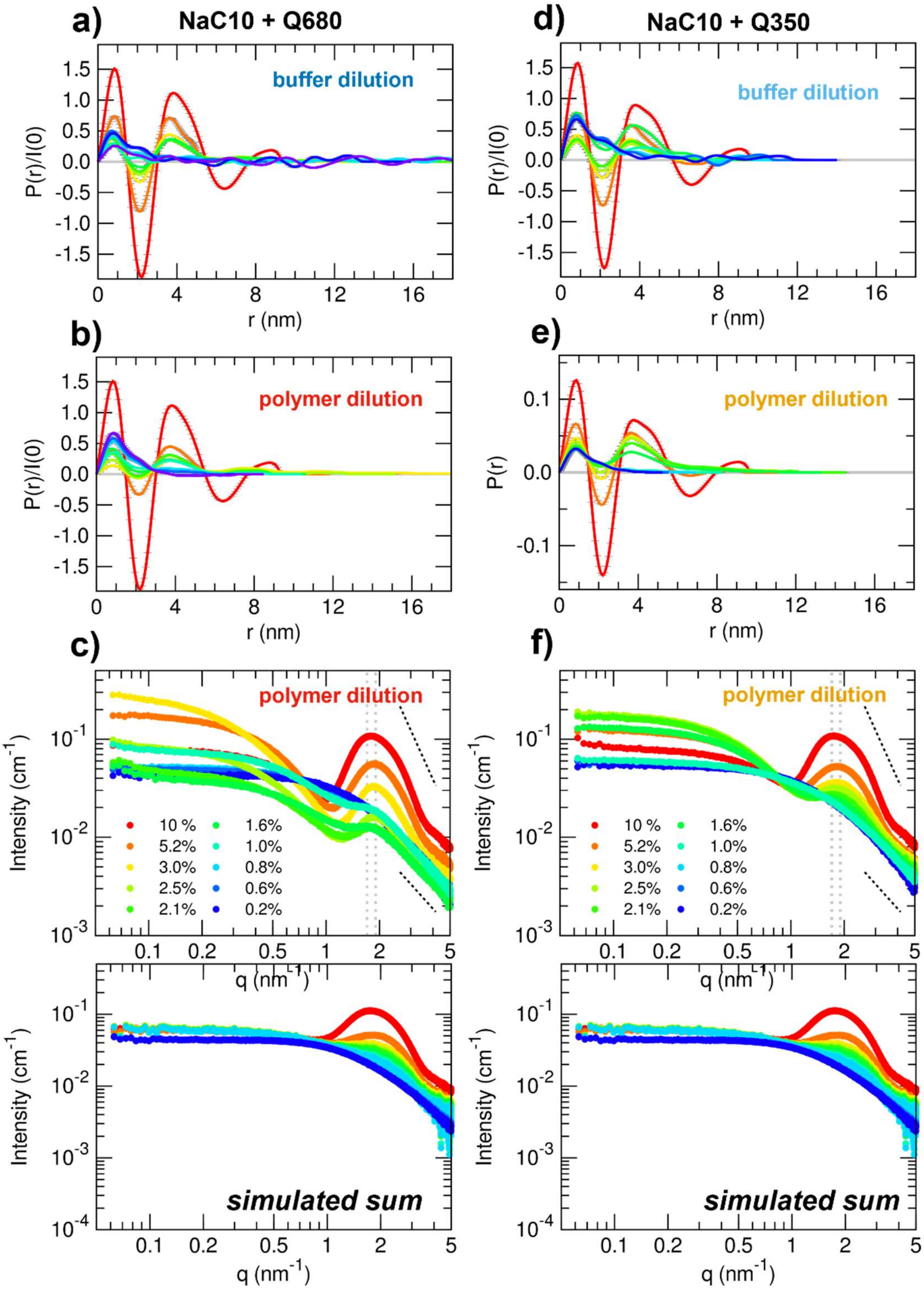

Figure A3. *Pair distance distribution functions (normalized by the I(0)) obtained by IFT of the SAXS data of mixtures in dilutions series, according to the colour code reported in Figure 4 in the main text. Simulated data of mixtures in the polymer dilution series as a simple sum of surfactant and polymer components, compared with the experimental trend of scattering profiles.*

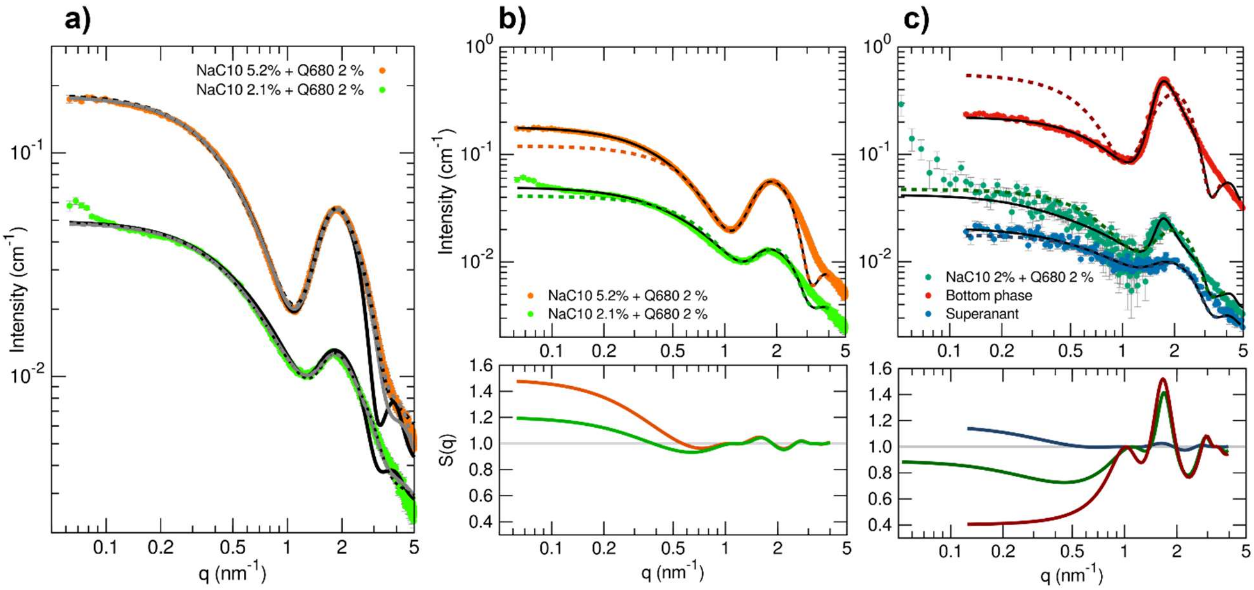

Figure A4. *a) SAXS patterns at 25 °C of the NaC10-Q680 2wt% mixtures with NaC10 concentration above and within the coacervation region shown in Figure 5a-b of the main text (colored dots), compared with model profiles obtained considering a monodisperse core-shell sphere model with sticky hard sphere structure factor (black solid line), a monodisperse core-shell ellipsoid model with sticky hard sphere structure factor (grey solid line), and polydisperse core-shell sphere form factors with sticky hard sphere structure factor (dotted lines) considering the SLD of the shell to be fixed (black) or free to be optimized (grey). b) For the model profiles reported in Figure 5a-b of the main text, the colored dashed lines show the form factor contribution, while the solid lines in the panel below represent the structure factor contribution. c) The same is reported for the data shown in Figure 5c of the main text.*

Table A.1. *Summary of SAXS data acquisition information, sample details, and data analysis software used.*

(a) Sample details for the SAXS experiments	
Concentration range (wt %)	
NaC10	*10-0.2*
quaternary ammonium inulin	*2-0.04*
Storage and dilution buffer composition	20 mM Tris pH 9, NaCl 0.525 wt%
(b) SAXS data collection parameters - Lab	
Source, instrument	SAXSLab Ganesha (JJXRay, now Xenocs)
Detector	PILATUS 300K
Beam geometry (mm^2)	0.5 x 0.5
Wavelength (Å)	1.54
sample-to-detector distance (m)	0.2-1
q-measurement range (nm^{-1})	0.05-20
Absolute scaling method	water scattering I(0)= 0.01632 cm^{-1} at 20°C

	capillary thickness estimated from alignment scans
Capillary path length (mm)	1.5 (disposable)
Sample volume (µl)	150
Exposure time (s)	3600, 14400
Number of exposures	1
Sample temperature (ºC)	room temperature (20-25 °C)
(c) SAXS data collection parameters - Synchrotron	
Source, instrument	BM29 (ESRF)
Detector	PILATUS 2M
Beam geometry (mm^2)	0.2 x 0.2
Wavelength (Å)	0.99186
sample-to-detector distance (m)	2.813
q-measurement range (nm^{-1})	0.06-5.2
Absolute scaling method	water scattering I(0)= 0.01632 cm^{-1} at 20°C
Capillary path length (mm)	1
Sample volume (µl)	50
Exposure time (s)	1
Number of exposures	10
Extra flow time (s)	15
Sample temperature (ºC)	20°C
(e) Software employed for SAS data reduction, analysis, and interpretation	
Solvent subtraction, averaging and basic analysis (Guinier fit)	ATSAS 3.2
Indirect Fourier transform	BayesApp
Theoretical intensity calculations	SasView, Sasfit

Table A.2. *Details of the models and parameters used for obtaining the calculated model SAXS profiles related to pure NaC10 and quaternary ammonium inulin samples. Error estimates can be considered of ± 1 on the last shown digit. Parameters that have not been modified in the optimization are shown in grey colour.*

a)	Pure NaC10		
Model	Form factor: spherical shell (SASfit 0.94.11, model 3.1.4) structure factor: Hayter Penfold RMSA (SASfit 0.94.11, model 4.5.1) monodisperse approximation		
q range (nm^{-1})	0.07-2.2		
NaC10 wt%	**2**	**5**	**10**
Parameters			
N (number density, $10^{-7}nm^{-3}$)	1193	9406	26377
core radius r_{core} (nm)	1.32	1.349	1.364
shell thickness t (nm)	0.98	1.005	0.979
ΔSLD_{core} (nm^{-2})	-0.000283	-0.000283	-0.000283
ΔSLD_{shell} (nm^{-2})	9.00E-05	9.00E-05	9.00E-05

V_{core} (nm^3)	9.66	10.28	10.62	Calculated $V_{core} = \frac{4}{3}\pi r^3$
Hard Sphere radius (nm)	2.35	2.35	2.00	
Z (charge)	1	7	7	
η (volume fraction)	0.001	0.07	0.144	
T (K)	298.15	298.15	298.15	
salt conc. (M)	0.1	0.1	0.1	
ε_r	71.08	71.08	71.08	
Background (cm^{-1})	0	0	0.0032	

Model	Form factor: ellipsoidal shell (SASfit 0.94.11, model 8.6.3) structure factor: Hayter Penfold RMSA (model 4.5.1) background broad peak: generalized Gaussian1 amplitude (model 7.12.1)			
q range (nm^{-1})	0.07-5.0			
NaC10 wt%	**1**	**2**	**5**	
Parameters				
N (number density, 10^{-7}nm^{-3})		1585.93	13541.6	
polar core radius r_{pol} (nm)		2.15	1.975	
equatorial core radius r_{eq} (nm)		1.025	1.071	
shell thickness t (nm)		0.940	0.946	
SLD_{core} (nm^{-2})		0.000657	0.000657	
SLD_{shell} (nm^{-2})		0.001030	0.001030	
$SLD_{solvent}$ (nm^{-2})		0.000940	0.000940	
V_{core} (nm^3)		9.46	9.49	Calculated $V_{core} = \frac{4}{3}\pi {r_{eq}}^2 r_{pol}$
Hard Sphere radius (nm)		3	2.20	
Z (charge)		7	7	
η (volume fraction)		0.0057	0.06	
T (K)		298.15	298.15	
salt conc. (M)		0.1	0.1	
dielectric constant ε_r		71.08	71.08	
Amplitude	0.0005	0.0009	0.001	
location (nm^{-1})	3.53	4.5	4.5	
scale or width	2.555	2.555	2.555	
shape (when =2 is Gaussian)	3.0	2.972	2.972	
background	0.0002	0.00017	0.0015	

b)	Pure Q680					
Model	Form factor: Generalized Gaussian coil (SASfit 0.94.11, model 8.4.1.5) structure factor: Hayter Penfold RMSA (SASfit 0.94.11, model 4.5.1) monodisperse approximation					
q range (nm^{-1})	0.07-5.0					
Q680 wt%	**2**	**1**	**0.5**	**0.2**	**0.1**	**0.04**
Parameters						
Free Flory exponent						
R_g (nm)	1.043	1.175	1.261	1.311	1.374	1.227
Flory exponent	0.45	0.48	0.51	0.52	0.60	0.42
I(0) (cm^{-1})	0.0475	0.0267	0.0145	0.0060	0.0033	0.0010
Hard Sphere radius (nm)	3.07	3	3	3	3	3
Z (charge)	6	6	6	6	6	6
η (volume fraction)	0.0086	0.00433	0.00217	0.0009	0.00045	0.00017
T (K)	298.15	298.15	298.15	298.15	298.15	298.15
salt conc. (M)	0.1	0.1	0.1	0.1	0.1	0.1
dielectric constant ε_r	71.08	71.08	71.08	71.08	71.08	71.08

Flory exponent=0.5						
R_g (nm)	1.058	1.171	1.233	1.284	1.285	1.573
Flory exponent	0.5	0.5	0.5	0.5	0.5	0.5
I(0) (cm^{-1})	0.0489	0.0269	0.014	0.00597	0.00298	0.00112
Hard Sphere radius (nm)	3	3	3			
Z (charge)	6	6	5			
η (volume fraction)	0.0094	0.0043	0.0022			
T (K)	298.15	298.15	298.15			
salt conc. (M)	0.1	0.1	0.1			
dielectric constant ε_r	71.08	71.08	71.08			
Flory exponent=0.5 and fixed R_g						
R_g (nm)	1.28			1.28		
Flory exponent	0.5			0.5		
I(0) (cm^{-1})	0.060			0.006		
Hard Sphere radius (nm)	1					
Z (charge)	4					
η (volume fraction)	0.0107					
T (K)	298.15					
salt conc. (M)	0.1					
dielectric constant ε_r	71.08					

c)	Pure Q350					
Model	Form factor: Generalized Gaussian coil (SASfit 0.94.11, model 8.4.1.5) structure factor: RPA S(q)=1/(1+νP(q)) (SASfit 0.94.11)					
q range (nm^{-1})	0.07-5.0					
Q350 wt%	**2**	**1**	**0.5**	**0.2**	**0.1**	**0.04**
Parameters						
Free Flory exponent						
R_g (nm)	1.070	1.174	1.247	1.28	1.25	1.25
Flory exponent	0.50	0.51	0.54	0.53	0.42	0.40
I(0) (cm^{-1})	0.0564	0.0310	0.0167	0.0068	0.0033	0.0012
ν						
Flory exponent=0.5						
R_g (nm)	1.17	1.25		1.25		
Flory exponent	0.5	0.5		0.5		
I(0) (cm^{-1})	0.0668	0.0366		0.0067		
ν	0.18	0.19				
Flory exponent=0.5 and fixed R_g						
R_g (nm)	1.25	1.25	1.25	1.25	1.25	1.25
Flory exponent	0.5	0.5	0.5	0.5	0.5	0.5
I(0) (cm^{-1})	0.079	0.036	0.017	0.0067	0.0034	0.0013
	0.41	0.18	0.06			

Table A.3. *Summary of the parameters used to calculate the model SAXS profiles related to mixtures of NaC10 and Quatin680. Parameters that have not been modified in the optimization are shown in grey colour.*

Sample	**Sample changer**	**Sample changer**	**Disposable Cap.**	**Phase Separated - supernatant**	**Phase separated – bottom**
NaC10 (wt%)	**5.2**	**2.1**	**2**	**(2)**	**(2)**
Q680 (wt%)	**2**	**2**	**2**	**(2)**	**(2)**

a)	
Model	spherical shell (SASfit 0.94.11, model 3.1.4) with sticky hard sphere S(q) (model 11.4.1)

	+ Generalized Gaussian coil (model 8.4.1.5) and broad peak background (model 7.12.1)				
q range (nm^{-1})	0.07-5.0				
Core-shell sphere P(q) with sticky hard sphere S(q)					
N (number density, $10^{-7}nm^{-3}$)	9751	1380	2969	1491	78355
core radius r_{core} (nm)	1.349	1.34	1.34	1.34	1.34
shell thickness t (nm)	1.16	1.13	1.01	0.90	1.06
ΔSLD_{core} (nm^{-2})	-0.000283	-0.000283	-0.000283	-0.000283	-0.000283
ΔSLD_{shell} (nm^{-2})	0.00011	0.00013	0.00013	0.00012	0.00011
Hard Sphere radius (nm)	2.5	2.46	2.30	2.44	2.24
τ (stickiness)	0.05	0.16	0.10	0.05	0.25
f_p (volume fraction)	0.011	0.08	0.40	0.009	0.39
Gaussian coil					
R_g (nm)	1.28	1.28	1.28	1.28	1.28
Flory exponent	0.5	0.5	0.5	0.5	0.5
I(0) (cm^{-1}) (0.06 for pure Q680 2%)	0.0298	0.0173	0.0197	0.0128	0.0911
Background					
Amplitude	0.0001	0.001	0.0007	0.0002	6.9E-07
location (nm^{-1})	4.5	4.5	4.5	4.5	4.5
scale or width	2.56	2.56	2.56	2.56	2.56
shape	2.97	2.97	2.97	2.97	2.97
background	0.0019	0.0010	0.0020	0.0016	0.030

b)

Model	ellipsoidal shell (SASfit 0.94.11, model 8.6.3) with sticky hard sphere S(q) (model 11.4.1) + Generalized Gaussian coil (model 8.4.1.5) and broad peak background (model 7.12.1)	
q range (nm^{-1})	0.07-5.0	
Core-shell ellipsoid P(q) with sticky hard sphere S(q)		
N (number density, $10^{-7}nm^{-3}$)	14053	1983
polar core radius r_{pol} (nm)	1.97	2.15
equatorial core radius r_{eq} (nm)	1.07	1.03
shell thickness t (nm)	1.115	1.110
SLD_{core} (nm^{-2})	0.000657	0.000657
SLD_{shell} (nm^{-2})	0.0010399	0.00105274
$SLD_{solvent}$ (nm^{-2})	0.00094	0.00094
Hard Sphere radius (nm)	2.28	2.16
τ (stickiness)	0.11	0.16
f_p (volume fraction)	0.04	0.09
Gaussian coil		
R_g (nm)	1.279	1.279
Flory exponent	0.5	0.5
I(0) (cm^{-1}) (0.06 for pure Q680 2%)	0.0306	0.0183
Background		
Amplitude	0.0020	0.0020
location (nm^{-1})	4.5	4.5
scale or width	2.555	2.555
shape	2.972	2.972
background	0.0009	2.81E-06

c)

Model	spherical shell (SASfit 0.94.11, model 3.1.4) with Lognormal polydispersity of the core radius and with sticky hard sphere S(q) (model 11.4.1)

+ Generalized Gaussian coil (model 8.4.1.5) and flat background		
q range (nm^{-1})	0.07-3.5	
Core-shell sphere P(q) with sticky hard sphere S(q)		
N (number density, $10^{-7}nm^{-3}$)	24359	5372
core radius $<r_{core}>$ (nm)	1.084	0.933
width r_{core} distribution	0.20	0.25
shell thickness t (nm)	1.16	1.25
ΔSLD_{core} (nm^{-2})	-0.000283	-0.000283
ΔSLD_{shell} (nm^{-2})	9.00E-05	9.00E-05
Hard Sphere radius (nm)	2.23	2.18
τ (stickiness)	0.14	0.19
f_p (volume fraction)	0.07	0.17
Gaussian coil		
R_g (nm)	1.278	1.278
Flory exponent	0.5	0.5
I(0) (cm^{-1})	0.0004	0.007
(0.06 for pure Q680 2%)		
Background		
background	0.0019	0.0010

Table A.4. *Estimate of the average molecular weight of quaternary ammonium inulin samples from the SAXS intensity extrapolated at zero angle. a) assumed mass and volumes based on the chemical structure. b) Calculations of molecular weight (M_W) and polymerization degree (n) based on the experimental values of I(0) according to equation A.1. The values obtained by Guinier fit for the samples with mass concentration greater than 0.2 wt% were not considered in the average due to possible influence of a repulsive structure factor.*

a)

	Partial Molar Volume cm³/mol	M_W g/mol	$\tilde{\upsilon}$ cm³/g	Molecular Volume nm³	Z (el.)	d (g/cm³)
covolume	12.4			0.021		
First glucose unit	107.9	179.14	0.602	0.179	95	1.660
Fructose unit cationic	213.2	280.33	0.761	0.354	153	1.315
Fructose unit cationic with Cl-	222.4	315.79	0.704	0.369	171	1.420
Frucose unit	99.5	163.15	0.610	0.165	87	1.640
Inulin	97.4	162.100	0.601	0.162		1.664

As a sum of units (including covolume and first glucose unit)

	Cationic fraction	N units	Vol. (nm3)	Mass (g/mol)	$\tilde{\upsilon}$ (cm³/g)	d (g/cm³)	Z (el.)	e/g	SLD (cm^{-2})	$\Delta\rho_M^2$ (cm^2/g^2)
Q680 - no Cl-	0.700	15	4.66	3857	0.728	1.374	2093	3.27E+23	1.27E+11	5.61E+020
Q350 - no Cl-	0.360	15	3.70	3259	0.683	1.464	1756	3.25E+23	1.34E+11	7.41E+020
Q680 - with Cl-	0.700	15	4.82	4229	0.687	1.457	2282	3.25E+23	1.33E+11	7.31E+020
Q350 - with Cl-	0.360	15	3.96	3552	0.671	1.491	1912	3.24E+23	1.36E+11	8.01E+020

Only fructose, weighted average of single monomer

	Cationic fraction	N units	Vol. (nm³)	Mass (g/mol)	$\tilde{\upsilon}$ (cm³/g)	d (g/cm³)	<Z>	e/g	SLD (cm^{-2})	$\Delta\rho_M^2$ (cm^2/g^2)
Q680 - no Cl-	0.700	1	0.297	245.2	0.730	1.369	133.2	3.27E+23	1.26E+11	5.54E+020
Q350 - no Cl-	0.360	1	0.233	205.3	0.684	1.462	110.8	3.25E+23	1.34E+11	7.42E+020

b)

C (wt%)	without Cl- (wt%)	conc. (g/cm^3)	R_g (nm)	err (nm)	$I(0)$ (cm^{-1})	err (cm^{-1})	M_W (Da)	err (Da)	n	n err
Q680										
Guinier fit in the q range (0.67-1.09) nm^{-1}										
0.039	0.036	0.0004	1.291	0.064	1.03E-03	5E-05	3077	135	12.6	0.55
0.104	0.095	0.0010	1.150	0.019	2.98E-03	4E-05	3360	40	13.7	0.16
0.208	0.190	0.0019	1.156	0.015	5.64E-03	5E-05	3183	29	13.0	0.12
0.503	0.458	0.0046	1.161	0.016	1.40E-02	1E-04	3279	33	13.4	0.13
1.004	0.915	0.0092	1.103	0.006	2.62E-02	1E-04	3070	11	12.5	0.05
1.998	1.822	0.0182	0.963	0.005	4.66E-02	1E-04	2746	7	11.2	0.03
Model fit with S(q)										
0.208	0.190	0.0019	1.279	0.008	0.006	0.0006	3358	332	13.7	1.4
1.998	1.822	0.0182	1.279	-	0.060	0.002	3543	109	14.5	0.4
Average							3304		13.5	
Stdev							180		0.7	
Q350										
Guinier fit in the q range (0.67-1.09) nm^{-1}										
0.041	0.038	0.0004	1.261	0.049	1.26E-03	4E-05	2710	117	13.2	0.57
0.107	0.098	0.0010	1.214	0.018	3.27E-03	4E-05	2715	41	13.2	0.20
0.205	0.188	0.0019	1.162	0.019	6.50E-03	8E-05	2806	44	13.7	0.22
0.508	0.466	0.0047	1.128	0.006	1.61E-02	6E-05	2803	13	13.6	0.07
1.000	0.917	0.0092	1.097	0.007	3.04E-02	1E-04	2688	15	13.1	0.07
2.000	1.835	0.0184	1.004	0.005	5.57E-02	1E-04	2465	8	12.0	0.04
Model fit with S(q)										
0.205	0.188	0.0019	1.25	0.01	0.007	0.001	2882	355	14.0	1.7
2.000	1.835	0.0184	1.25	-	0.079	0.002	3516	75	17.1	0.4
Average							2926		14.2	
Stdev							338		1.6	

Table A.5. *Thickness, solvent content, composition, and adsorbed mass of the layers of the models that best fit the experimental neutron reflectometry data.*

	Bare surface	**After buffer dilution**	**After polymer dilution**
SiO_2 thickness (nm)	0.9 ± 0.2	0.9 ± 0.2	0.9 ± 0.2
Solvent (v/v)	0.05 ± 0.005	0.01 ± 0.005	0.01 ± 0.005
Layer 1 thickness (nm)	-	1.2 ± 0.3	3.1± 0.2
Layer 1 Solvent (v/v)	-	0.75 ± 0.01	0.81 ± 0.01
Layer 1 Polymer (v/v)	-	0.95± 0.15	0.98 ± 0.15
Adsorbed mass (mg/m^2)	-	0.49	0.85

References

[1] T. Zemb, P. Charpin, Micellar Structure From Comparison Of X-Ray And Neutron Small-Angle Scattering., J. Phys. Paris. 46 (1985) 249–256. https://doi.org/10.1051/jphys:01985004602024900.

[2] E. Vikingstad, A. Skauge, H. Høil and, Partial molal volumes and compressibilities of the homologous series of sodium alkylcarboxylates, R6COONaR13COONa, in aqueous solution, J. Colloid Interface Sci. 66 (1978) 240–246. https://doi.org/10.1016/0021-9797(78)90301-6.

[3] R. De Lisi, G. Perron, J.E. Desnoyers, Volumetric and thermochemical properties of ionic surfactants: sodium decanoate and octylamine hydrobromide in water, Can. J. Chem. 58 (1980) 959–969. https://doi.org/10.1139/v80-152.

[4] S.M. Calderón, N.L. Prisle, Composition dependent density of ternary aqueous solutions of ionic surfactants and salts: Capturing the effect of surfactant micellization in atmospheric droplet model solutions, J. Atmos. Chem. 78 (2021) 99–123. https://doi.org/10.1007/s10874-020-09411-8.

[5] M.T. Ivanović, M.R. Hermann, M. Wójcik, J. Pérez, J.S. Hub, Small-Angle X-ray Scattering Curves of Detergent Micelles: Effects of Asymmetry, Shape Fluctuations, Disorder, and Atomic Details, J. Phys. Chem. Lett. 11 (2020) 945–951. https://doi.org/10.1021/acs.jpclett.9b03154.

[6] K. Manalastas-Cantos, P. V. Konarev, N.R. Hajizadeh, A.G. Kikhney, M. V. Petoukhov, D.S. Molodenskiy, A. Panjkovich, H.D.T. Mertens, A. Gruzinov, C. Borges, C.M. Jeffries, D.I. Sverguna, D. Frankea, ATSAS 3.0: Expanded functionality and new tools for small-angle scattering data analysis, J. Appl. Crystallogr. 54 (2021) 343–355. https://doi.org/10.1107/S1600576720013412.

[7] S. Hansen, BayesApp : a web site for indirect transformation of small-angle scattering data, J. Appl. Crystallogr. 45 (2012) 566–567. https://doi.org/10.1107/S0021889812014318.

[8] H. Durchschlag, P. Zipper, Calculation of the partial volume of organic compounds and polymers, Springer-Verlag GmbH & Company KG, 1994. https://doi.org/10.1007/bfb0115599.

[9] H. Durchschlag, Thermodynamic Data for Biochemistry and Biotechnology, Springer-Verlag, Berlin - Heidelberg - New York - Tokyo, 1986. https://doi.org/10.1016/0302-4598(88)80044-8.